

# LASER-ASSISTED FORMATION OF HIGH-QUALITY POLYCRYSTALLINE DIAMOND MEMBRANES

V. S. Sedov,<sup>1\*</sup> A. A. Voronin,<sup>2</sup> M. S. Komlenok,<sup>1</sup> S. S. Savin,<sup>3</sup>  
A. K. Martyanov,<sup>1</sup> A. F. Popovich,<sup>1</sup> A. S. Altakhov,<sup>1</sup>  
A. S. Kurochka,<sup>2</sup> D. V. Markus,<sup>2</sup> and V. G. Ralchenko<sup>1</sup>

<sup>1</sup>*Prokhorov General Physics Institute, Russian Academy of Sciences  
Vavilova Str. 38, Moscow 119991, Russia*

<sup>2</sup>*JSC RPC "Istok" named after Shokin  
Fryazino, Moscow Region 141190, Russia*

<sup>3</sup>*MIREA Russian Technological University  
Prospect Vernadskogo 78, Moscow 119454, Russia*

\*Corresponding author e-mail: sedovvadim@yandex.ru

## Abstract

A polycrystalline diamond film is grown on a 2 inch Si substrate using a microwave-plasma chemical-vapor-deposition technique. The high quality of the diamond films is confirmed by Raman spectra. A multiple-step procedure is used for local etching of the substrate to form the pattern of an array of 50 diamond membranes with the diameter in a range from 150 to 300  $\mu\text{m}$ . The morphology of the membranes is examined using scanning electron microscopy. The membranes obtained can be used as the base material for the fabrication of pressure sensors, X-ray detectors and scintillators, and in quantum optics as optical resonators for single-color centers in diamond.

**Keywords:** polycrystalline diamond, chemical-vapor-deposition (CVD) technique, laser ablation, membranes, etching.

## 1. Introduction

Diamond as the material has a wide range of possible applications in biomedicine, electronic, and quantum optics [1]. For many of such applications, the thin transparent films with thickness in a range from 100 nm up to tens of micrometers are in demand rather than bulk freestanding materials. A film locally freed from a substrate is called the membrane. In this case, the preserved part of the substrate serves as a rigid frame to support such a fragile thin membrane.

The first application for diamond membranes was related to prospects of using them in X-ray lithography [2], as diamond has low absorption in the X-ray spectral region. The combination of diamond low absorption and high thermal conductivity allows the formation of tunable composite materials for the fabrication of X-ray detectors and sensors [3, 4]. Thin diamond membranes were used as the platform to fabricate optical resonator structures, enhancing the photoluminescence of single-color centers in diamond [5, 6], such as "nitrogen-vacancy" and "silicon-vacancy" color centers. The flexibility and the fracture strength [7] of polycrystalline diamond allows the fabrication of durable thin membranes to be used as pressure sensors [8], as well as diamond micro- and nanodevices [9].

To date, several approaches to the manufacture of polycrystalline diamond membranes have been developed. The general approach is to use standard lithography techniques for substrate removal [9, 10]. However, this approach requires to prepare an expensive template for each new pattern of membranes. An alternative approach that does not require any template is to use a focused ion beam (FIB) etching to remove the substrate or to cut a small membrane from the top of the diamond material. However, in both cases, only single membranes can be produced in a reasonable time. So, the adaptable and easy-to-use method for the fabrication of patterns of well-shaped diamond membranes is of high demand.

In this work, we propose and realize the laser-assisted method for the formation of high-quality polycrystalline diamond membranes in complex patterns over large-area samples with the diameter over 2 inches.

## 2. CVD Synthesis of Diamond Films

The general approach of our experiment is shown in Fig. 1. The chemical-vapor-deposition technique (CVD) was used to form a polycrystalline diamond film on a silicon substrate (1). To reduce the aspect ratio of holes, the substrate was homogeneously thinned to a thickness of  $150\ \mu\text{m}$  (2). The continuous aluminum mask was deposited on the bottom side of the Si substrate (3). The excimer laser was used to form windows in Al mask (4). The etching of Si was performed to locally remove the substrate with the diamond film being the stop-layer for the etching process (5). As a result, a pattern of diamond membranes on the Si substrate has been formed (6).

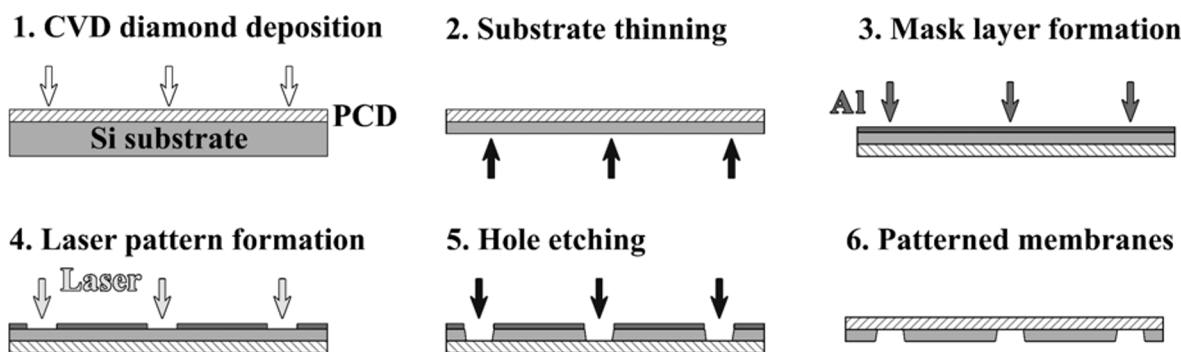


**Fig. 1.** The scheme of the patterned diamond-membrane preparation (cross-section view).

Thus, in the first step, a high-quality polycrystalline diamond film was synthesized on a silicon substrate. A  $400\ \mu\text{m}$  thick polished 2 inch single crystal (111) Si substrate was seeded with nanodiamond (ND) particles using an ultrasonic treatment for 10 min in a water-based suspension of the ND powder with the average size of 5 nm (Daicel) to provide diamond nucleation centers. The substrate was dried in air using spin-coater SPIN150 (2000 rpm, 10 min) to form a homogeneous seeding layer with nucleation density over  $10^9\ \text{cm}^{-2}$ .

Polycrystalline diamond films were put in a microwave-plasma chemical-vapor-deposition (MPCVD) system ARDIS-100 (2.45 GHz, Optosystems Ltd) in  $\text{CH}_4/\text{H}_2$  gas mixtures with the methane content of 6%. Other process parameters were the following: total gas flow of 500 sccm, gas pressure 55 Torr, microwave power 5 kW, substrate temperature  $800^\circ\text{C}$  as measured with a two-color pyrometer (Micron M770). The deposition time was 8 h. The film thicknesses and growth rate were controlled with

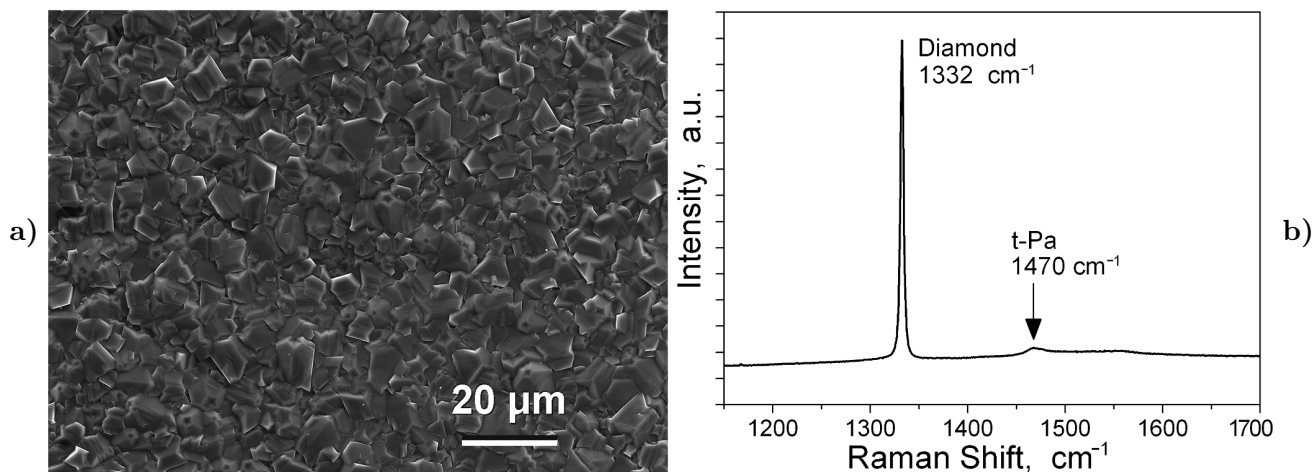


**Fig. 2.** Polycrystalline diamond film deposited on the Si substrate. Here, SEM image of the surface and (a) and Raman spectrum (average of 10 spectra taken from random areas of the sample) (b).

laser interferometry. As a result of CVD growth, the continuous 12  $\mu\text{m}$  thick polycrystalline diamond layer was formed on the top side of the Si substrate, which was confirmed using scanning electron microscopy (TESCAN MIRA3; see Fig. 2 a). The film consisted of randomly-oriented well-faceted diamond grains with sizes of 5 – 10  $\mu\text{m}$ .

The phase composition of the obtained film was analyzed at room temperature with micro-Raman spectroscopy using LABRAM HR-800 spectrometer equipped with a diode-pumped solid-state laser ( $\lambda = 473 \text{ nm}$ ). The spectrometer operated in a confocal mode, while the laser beam was focused in a spot of  $\approx 1 \mu\text{m}$  in diameter of the sample surface. The sharp 1st-order diamond Raman peak at  $1332.0 \text{ cm}^{-1}$  with the full width at half maximum (FWHM) of  $4.0 \text{ cm}^{-1}$  was observed in the spectrum of the film (Fig. 2 b), as well as a weak band of trans-polyacetylene (t-PA) at  $1470 \text{ cm}^{-1}$ , which is a common impurity located in grain boundaries of polycrystalline diamond films. No signs of D- and G-bands ( $1350 \text{ cm}^{-1}$  and  $1590 \text{ cm}^{-1}$ , correspondingly) of the graphitic  $\text{sp}^2$  phase were observed, which confirms the high quality of the deposited film.

### 3. Fabrication of Membranes

For the convenience of the upcoming selective etching procedure, the Si substrate was thinned to a thickness of 150  $\mu\text{m}$  by the means of mechanical polishing in Logitech MP5 automated system, using quartz grinding disc and watering with a suspension of diamond powder. After the thinning process, the sample was briefly etched in a 1% solution of fluoric acid (HF) in water for 1 min and then cleaned in deionized water. The metallic 0.1  $\mu\text{m}$  thick Ti sublayer and the 2  $\mu\text{m}$  thick Al mask layer were formed on the bottom side of the Si substrate using electron-beam physical vapor deposition (Evotec BAK 761, substrate temperature  $150^\circ\text{C}$ ).

The group of holes in the Al layer was fabricated using excimer KrF laser CL-7100 (Optosystems Ltd., CL 7100, wavelength  $\lambda = 248 \text{ nm}$ , pulse duration  $\tau = 20 \text{ ns}$ , and repetition rate  $f = 50 \text{ Hz}$ ). The irradiation of the sample was carried out using a projection scheme, which reduced the size of the mask by 20 times. Seven separate tantalum masks with circle-shaped 3–6 mm windows in their centers were

used to cut the central part of the laser spot; therefore, the spot with uniform energy distribution on the irradiated surface was formed, and its diameter was changed discretely from 150 to 300  $\mu\text{m}$  with a step of 25  $\mu\text{m}$ . Laser fluence was 1.5  $\text{J}/\text{cm}^2$  and exceeded the ablation threshold of aluminum and silicon. The number of pulses was 20, which was enough to drill the aluminum film through and slightly ablate the silicon substrate to ensure the removal of the protective metal layer. At the end of metal drilling, local heat is mainly dissipated into the silicon substrate to the heat diffusion length  $\sigma = (\chi \cdot \tau)^{1/2} \approx 130$  nm, where Si heat diffusivity  $\chi = 0.9$   $\text{cm}^2/\text{s}$ .

The optical absorption coefficient  $\alpha_{\text{Si}}$  is  $1.8 \cdot 10^6$   $\text{cm}^{-1}$  [11] and corresponds to the optical absorption length of 6 nm. The calculated values of the heat diffusion and optical absorption lengths are much smaller than the thickness of the silicon substrate, and therefore the laser ablation of the Al/Ti layer does not affect the diamond film. The sample was mounted onto a translation stage that allowed us to shift the laser spot over the surface. The lateral positions of the drilled windows on the sample were determined by the programming of the stage, while the diameter and the shape of each window were determined by the appropriate choice of the mask for the laser beam. The total number of 50 separate windows was formed by this technique. The distance between the windows was 5 mm. After the laser drilling process, a 1% HF solution was used to remove a layer of residual  $\text{SiO}_2$  from the surface of the Si substrate in the etched region.

The plasma Si etching was used to selectively etch substrate through the windows in the Al mask from the bottom side up to the diamond layer. There was almost no chemical etching of the Al layer by plasma, so only Si areas under the windows in the mask were etched. The isopropanol was used for sample cleaning as the very final step of the diamond membrane preparation.

Plasma-chemical etching through the silicon substrate was performed using the inductively-coupled plasma (ICP) with the PLASMA TM5 installation (13.56 MHz). Etching mode:  $\text{SF}_6$  gas feed of 6 l/min, Ar gas feed of 4 l/min, pressure 6 Pa, inductor power 300 W, and lower electrode power 40 W. The overall etching rate was at 5  $\mu\text{m}/\text{min}$ . The depth of etching was monitored using a Dektak 150 profilometer.

The formation of membranes was confirmed by the SEM investigation of both sides of the sample. On the bottom side of the Si substrate a series of holes were observed (Fig. 3). In Fig. 3 a, we show a case of the partly-formed surface of the diamond membrane (bottom side). Out of 50 membranes, only 3 were

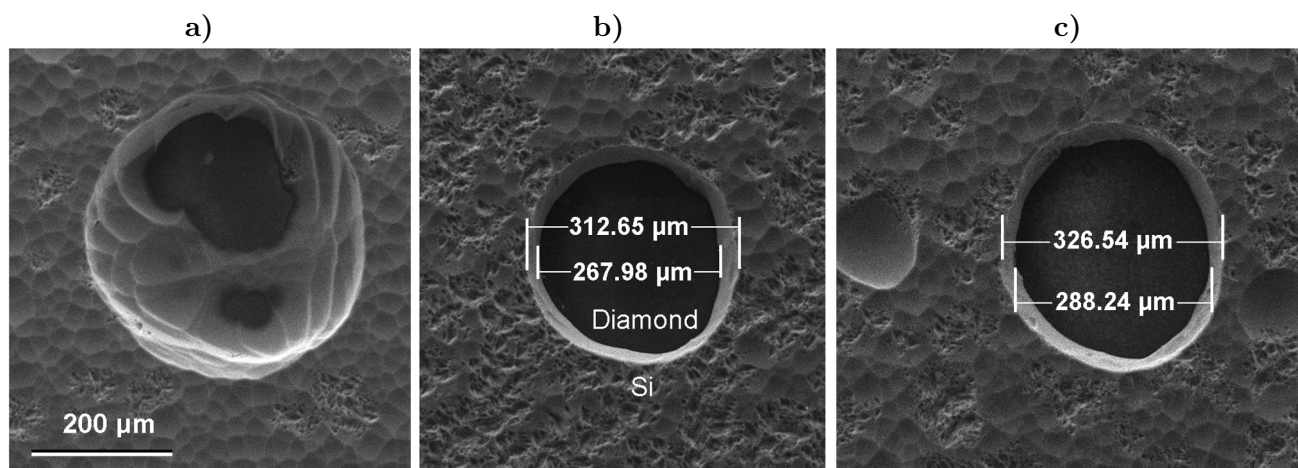


**Fig. 3.** SEM images of formed diamond membranes from the bottom side. Here, partly-formed membrane (a) and two typical fully-formed membranes with diameters of 268  $\mu\text{m}$  (b) and 288  $\mu\text{m}$  (c).

partly-formed and 2 more were damaged, while the majority of the membranes were well-shaped and fully-formed (see Fig. 3 b and c). The difference between the radius of the window in the Al mask and the resulting radius of the membrane was  $\sim 20 \mu\text{m}$ . Thus, considering the thickness of the etched Si layer to be  $150 \mu\text{m}$ , the tilt angle of hole sidewalls was estimated at  $7.7^\circ$ , which allows the formation even more complex patterns and shapes of the resulting diamond membranes, even with high aspect ratio.

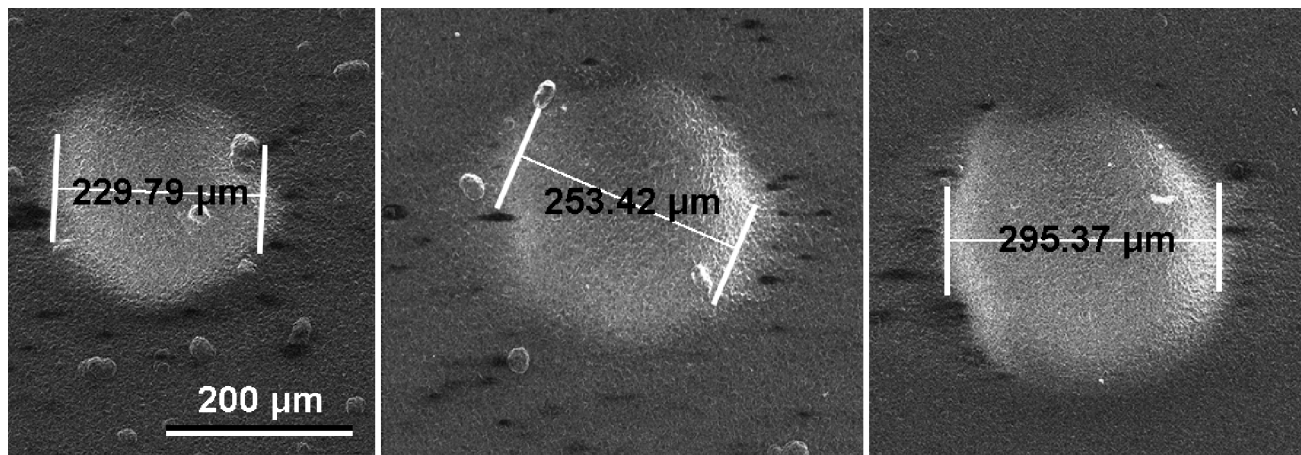


**Fig. 4.** SEM images of the growth surface of the polycrystalline diamond film – three diamond membranes with diameters of 230, 253, and 295  $\mu\text{m}$  are visible due to the charging effect.

The surface of the diamond film was found to be nearly unaffected by the membrane formation procedure. Still, overviewing the sample with low magnification, we observed a series of bright spots (Fig. 4). The pattern formed by these bright spots follows the pattern of windows in the Al mask on the bottom side of the sample. The size of such spots is  $200 - 300 \mu\text{m}$ , which is very close to the size of the formed membranes. Thus, the formed membranes can be directly observed from the surface of the diamond film due to the effect of charge accumulation in areas, where relatively conducting Si layer was removed from underneath the diamond film. No wrinkling of the membranes was observed. The majority ( $\sim 80\%$ ) of the membranes were well-shaped and pinhole-free. Thus, both the high quality of diamond material and the desirable structure of membranes were confirmed.

## 4. Summary

The new approach to the formation of polycrystalline diamond membranes was realized with the combination of chemical-vapor deposition of diamond, laser patterning of Al mask, and selective plasma chemical etching of silicon substrate. The  $12 \mu\text{m}$  thick polycrystalline diamond membranes with diameters of  $230 - 300 \mu\text{m}$  were prepared and investigated. The formation process preserved the desirable shape of the membranes. The tilt angle of hole sidewalls was estimated at  $7.7^\circ$ . The majority of membranes showed no signs of wrinkling, damage, or residual Si on the substrate side. Such membranes can be used as the base material for the fabrication of pressure sensors, X-ray detectors and scintillators, and in quantum optics as optical resonators for single color centers in diamond.

## Acknowledgments

The authors thank Daicel Corporation for providing high-density nanodiamond slurries. The work was supported by the Russian Science Foundation under Grant No. 19-72-00194.

## References

1. L. S. Pan and D. R. Kania, *Diamond: Electronic Properties and Applications*, Springer Science & Business Media (2013).
2. H. Windischmann and G. F. Epps, *J. Appl. Phys.*, **68**, 5665 (1990).
3. V. S. Sedov, S. V. Kuznetsov, V. G. Ralchenko, et al., *Diam. Relat. Mater.*, **72**, 47 (2017).
4. V. Sedov, S. Kouznetsov, A. Martyanov, et al., *ACS Appl. Nano Mater.*, **3**, 1324 (2020).
5. C. F. Wang, R. Hanson, D. D. Awschalom, et al., *Appl. Phys. Lett.*, **91**, 201112 (2007).
6. A. Schmidt, J. Bernardoff, K. Singer, et al., *Physica Status Solidi A*, **216**, 1900233 (2019).
7. V. G. Ralchenko, E. Pleuler, F. X. Lu, et al., *Diam. Relat. Mater.*, **23**, 172 (2012).
8. S. Drijkoningen, S. D. Janssens, P. Pobedinskas, et al., *Sci. Rep.*, **6**, 1 (2016).
9. S. D. Janssens, D. Vazquez-Cortes, A. Giussani, et al., *Diam. Relat. Mater.*, **98**, 107511 (2019).
10. M. E. Belousov, E. A. Il'ichev, A. E. Kuleshov, et al., *Tech. Phys. Lett.*, **38**, 225 (2012).
11. M. A. Green and M. J. Keevers, *Prog. Photovolt. Res. Appl.*, **3**, 189 (1995).